Development of a Variable Stiffness and Damping Tunable Vibration Isolator

JOHAN M. CRONJÉ
Dynamic Systems Group, Department of Mechanical and Aeronautical Engineering, University of Pretoria, South Africa, PO Box 11334, Erasmuskloof, 0048, South Africa (johanm.cronje@kentron.co.za)

P. STEPHAN HEYNS
NICO J. THERON
Dynamic Systems Group, Department of Mechanical and Aeronautical Engineering, University of Pretoria, Pretoria, 0002, South Africa

PHILIP W. LOVEDAY
Manufacturing and Materials Technology, Council for Scientific and Industrial Research (CSIR), Pretoria, South Africa, PO Box 395, Pretotia, 0001, South Africa

(Received 25 July 2003; accepted 6 August 2004)

Abstract: In this paper we report on the development of a variable stiffness and damping Liquid Inertia Vibration Eliminator (LIVE) vibration isolator. The result is the ability to shift the isolation frequency of the isolator and also to change the amplification at resonance. A practical variable stiffness spring was developed by using a compound leaf spring with circular spring elements. A wax actuator, controlled by a hot-air gun with a closed-loop displacement and velocity feedback control system, was used to separate the springs at the center. An experimental isolator was constructed and tested. The isolation frequency was shifted from 22.8 to 36.2 Hz by changing the stiffness of the spring by 270%. A transmissibility of less than 10% was achieved over the whole range. The viscous damping ratio was changed from 0.001 to 0.033 by increasing the flow losses in the system.

Key Words: Tunable vibration isolator, liquid inertia vibration eliminator, variable stiffness spring, wax actuator

1. INTRODUCTION

Vibrating machines such as rock-drills, compactors, and vibrating screens can cause serious damage to foundations and structures and may also cause injuries to operators. For this reason it is sometimes necessary to isolate the vibration of these machines from their surroundings. The vibration of many such machines is dominated by its response at the operating frequency. This raises the possibility of using tuned vibration absorbers to act as vibration isolators and to attenuate the vibration transmitted to the environment. An absorber utilized

Journal of Vibration and Control, **11:** 381–396, 2005 DOI: 10.1177/1077546305048585

in this capacity is referred to as a vibration isolating absorber, in contrast to conventional absorbers that are employed to enforce the low response of the primary system itself.

Conventional vibration isolators employ low-stiffness springs to accomplish vibration isolation, but this may lead to unacceptably large operational displacements. To counteract this problem, vibration-absorbing isolators that are tuned to specific excitation frequencies have been developed, and devices such as the Improved Rotor Isolation System (IRIS; Desjardins and Hooper, 1976, 1980) and the Dynamic Anti-Resonant Vibration Isolator (DAVI; Braun, 1980; Rita et al., 1976; Flannelly, 1966) have been in use for many years. These isolators react to the excitation forces of the source by their own inertia forces and can achieve almost perfect isolation at the isolation frequency if the damping is low. This can be done without the disadvantages of low stiffness and large static deflection that occur with conventional isolators. The practical utility of these isolators was significantly enhanced through the introduction of hydraulic amplification (Braun, 1980). This resulted in the development of the Liquid Inertia Vibration Eliminator (LIVE; Halwes, 1981; Halwes and Simmons, 1980) isolator.

The application of vibration absorbing isolators for machines where the response is dominated by the operating frequency is however hampered by the fact that the operating frequencies often change over time. For a LIVE isolator to adapt to such changes, it has to be able to shift its isolation frequency. It has been shown that this could be achieved by changing the port length (Smith and Stamps, 1995), port diameter (Smith and Stamps, 1998) or stiffness (Hodgson and Duclos, 1991) of the isolator.

In the current study, we have investigated the practical design of a variable stiffness device to change the isolation frequency of a LIVE isolator. The device comprises a compound leaf spring in which the leaves are separated by a wax actuator that is controlled by a closed-loop control system. The development and testing of the device is discussed and its ability to adapt to varying excitation conditions is demonstrated.

In the design of the system, one must take into account that perfect tonal excitation is seldom encountered in practice. There is usually some wide band vibration present. Since tuned absorbing isolators introduce their own natural frequencies into the new system, the vibration will be amplified at the natural frequencies of the isolator. If high levels of vibration are present at a frequency corresponding to a natural frequency, it becomes necessary to increase the damping of the isolator so as to decrease the amplification of the vibration at the natural frequency, and hence reduce the effective levels of vibration over the whole frequency range of interest.

2. LIVE ISOLATOR MODEL

The LIVE isolator concept is schematically illustrated in Figure 1. The transmissibility of such an isolator may be defined as the ratio between the output and the input displacements. Assuming incompressible flow and applying the principle of mass flow continuity, the transmissibility can be determined as a function of circular frequency. This equation originates in the equation of the transmissibility of the IRIS system (Desjardins and Hooper, 1976). Although the equation for the LIVE isolator was originally published by Halwes, the following nondimensionalized form of the equation is given instead (Du Plooy, 1999):

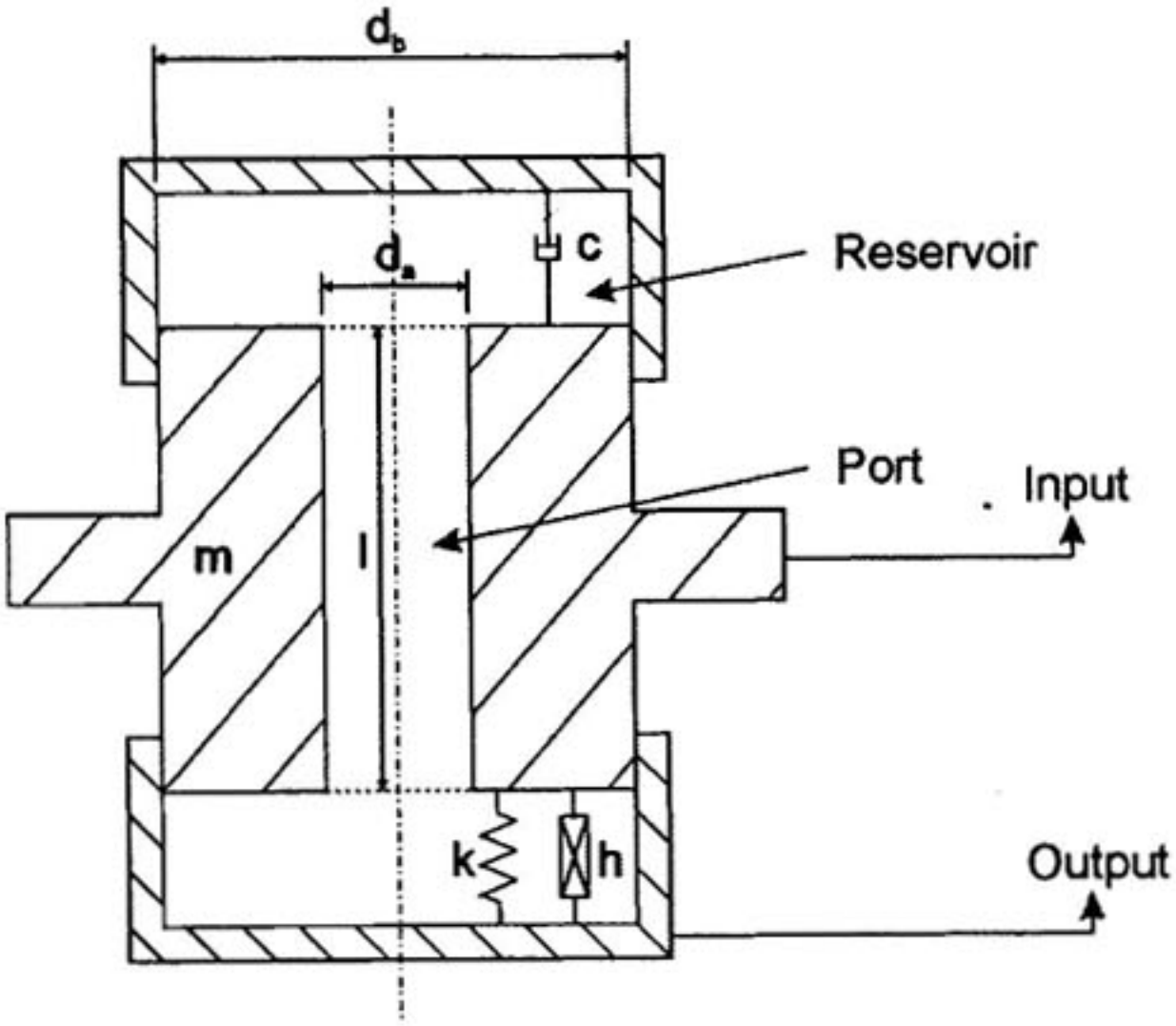

Figure 1. LIVE isolator.

$$|T_r| = \left\{ \frac{\left[1-(\omega/\omega_a)^2\right]^2 + \left[2\zeta(\omega/\omega_n)+\eta\right]^2}{\left[1-(\omega/\omega_n)^2\right]^2 + \left[2\zeta(\omega/\omega_n)+\eta\right]^2} \right\}^{1/2}, \tag{1}$$

with the undamped isolation frequency

$$\omega_a = \sqrt{\frac{-k}{m_b\left[1-(A_a/A_b)\right](A_a/A_b)}} \tag{2}$$

and the undamped natural frequency

$$\omega_n = \sqrt{\frac{k}{m + m_b\left[1-(A_b/A_a)\right]^2}}. \tag{3}$$

The absorber mass is

$$m_b = \rho \ell A_a. \tag{4}$$

Other parameters in these expressions are the viscous damping ratio ζ, the hysteretic loss factor η, and the fluid density ρ. The system geometry is defined by the port length ℓ, the port section area A_a and the reservoir section area A_b. The isolator stiffness coefficient is represented by k, and m denotes the isolator mass.

Equation (2) indicates that there are a few parameters which will influence the isolation frequency of the isolator. As some of these parameters are very difficult to change, such

as the reservoir area or fluid density, they will be ignored. From this, it follows that the port length, port diameter, and stiffness coefficient are the parameters that can be changed to influence the isolation frequency. Of these three parameters, the stiffness coefficient is the only one that will not influence the absorber mass. The effect of a change in absorber mass is a change in the degree of isolation achieved. The aim is to change the isolation frequency of the isolator. For the best performance, the lowest possible transmissibility should be achieved at the isolation frequency, regardless of what the isolation frequency is. If the absorber mass is altered, the transmissibility at the isolation frequency will increase as the isolation frequency decreases. Minimum transmissibility will therefore not be achieved at the isolation frequency. By changing the stiffness, only the isolation frequency will change and not the amount of isolation achieved at the isolation frequency. Minimum transmissibility will therefore be achieved at the isolation frequency, regardless of the set point of the isolation frequency. It is therefore appropriate to change the stiffness coefficient of the isolator in order to shift the isolation frequency.

3. VARIABLE STIFFNESS SPRINGS

Various attempts to develop variable stiffness springs for semi-active vibration absorbers are described in the literature. Walsh and Lamancusa (1992) describe a spring that can change its stiffness by 45 times by separating the two leaves of a compound leaf spring, albeit for a very low stiffness application. Longbottom and Rider (1987) proposed a concept based on a mass suspended between two air springs, whose stiffness could be changed by altering the pressure inside the air springs. This concept features the ability to achieve very low stiffness owing to the use of air springs. This concept was later improved by using a simple method of automatically adjusting the stiffness (Brennan et al., 1996).

Changing the number of active coils in a coil spring is an alternative way of making a variable stiffness spring (Franchek et al., 1995). By contrast, Ribakov and Gluck (1998) considered changing the angle at which a coil spring is oriented as a way of changing its effective stiffness. Smith (1991) proposed the heating of a temperature-dependent viscoelastic element to change its stiffness characteristics. Von Flotow et al. (1994) investigated electromagnetism as a means of influencing the stiffness of a spring and a variable stiffness spring that has primary coil springs whose stiffness is reduced by an electromagnetic negative stiffness. The use of shape memory alloys (SMAs) is another way to create a variable stiffness spring by turning the SMA wire into a coil spring (Siler and Demoret, 1996).

Most of these variable stiffness springs were developed for semi-active vibration absorbers and sometimes gave difficulties in practice. For application in a vibration isolator, the requirements for lateral stiffness and stroke length differ from those for a vibration absorber. In isolators, a high lateral stiffness is usually needed in order to transmit torques or forces through the spring to the primary system in the nonvibrating directions. A good example is a case where the isolator is inserted between a vibrating machine and the handle of the machine. The operator needs high lateral stiffness so that he can accurately control the machine while the isolator isolates the machine's vibrations from the handle in the vibrating direction. Lateral stiffness is usually not such a crucial parameter for vibration absorbers. In a vibration absorber, there is only a mass connected to the spring that is free to vibrate, so

no forces need to be transmitted to the primary system in the nonvibrating directions. Vibration absorbers are normally used in higher-frequency applications where the amplitudes of vibration are lower. Therefore, the stroke length of the spring is much smaller than is needed for the LIVE isolator. Because the isolator will be designed for lower frequencies, the stroke length will be much longer and the spring has to be able to cope with the high-amplitude vibrations.

The variable stiffness LIVE isolator developed by Hodgson and Duclos (1991) made use of an electrorheological fluid to change the dynamic stiffness of the isolator and did not use a variable stiffness spring. Therefore, a new spring was developed that could be practically implemented on a LIVE isolator.

In the course of this investigation the following specifications were found to be reasonably practical to physically realize.

- Stiffness change larger than 40%. The degree of stiffness change will determine the shift in isolation frequency. The larger the shift in isolation frequency, the more usable the isolator. A change of about 18% in isolation frequency corresponds to a 40% change in stiffness and will give the isolator a large enough frequency shift to allow it to be used in a variety of applications.
- Loss factor less than 0.15. It is possible to change the amount of damping of the system. For this change to be effective, the minimum damping of the system should not be too high. For this particular investigation a nominal loss factor value of 0.15 was found to be reasonably obtainable.
- Response time less than 30 s. The response time should ideally be as fast as possible. If the response time is too slow, the excitation conditions will change faster than the absorber can adapt to the changes, and will therefore not be effective. Although the isolator will not be designed for a specific application, a requirement of a response time less than 30 s was decided on after considering typical operating environments and possible actuation mechanisms. A response time of 30 s will not put an unrealistic constraint on the performance of the separation mechanism and will enable the system to respond effectively to slow changes in excitation conditions. The isolator will therefore not be intended to have a very fast response or to adapt to rapid changes in excitation conditions. It is intended for applications where the excitation conditions will change over a few minutes or hours, owing for example to variations in loads and other operating conditions.

The compound leaf spring concept was used as the basic working principle of the spring in this study, for the following reasons.

- The work by Walsh and Lamancusa (1992) shows that the concept has the capability of achieving a very large degree of stiffness change that will be ideal for varying the isolation frequency of an isolator.
- The all-steel construction of the spring will yield a spring with low structural damping that is also ideal for implementation on a LIVE isolator.
- A leaf spring can handle large displacements and will be suitable for large-amplitude vibrations.

Figure 2 shows the basic configuration of this concept, with two leaf spring elements separated at the center. As the two leaves are separated, the overall stiffness of the spring

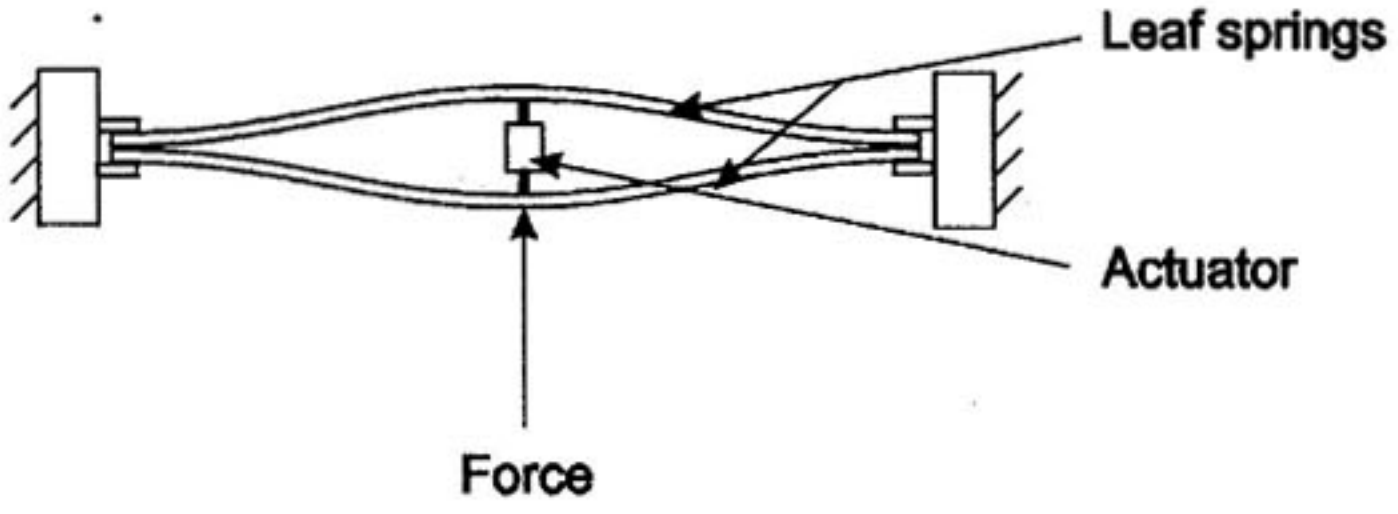

Figure 2. Basic configuration of compound leaf spring.

assembly is increased as a result of the nonlinearity of the springs. The nonlinearity is caused by geometrical changes as well as the elongation of the spring elements. These two mechanisms work together to achieve the resulting change in stiffness, with the elongation effect contributing most to the stiffening of the spring. The geometrical stiffening effect is due to the change in the geometrical form of the spring as the two leaves are separated. The geometrical form of the spring with the leaves separated is much stiffer than the relaxed form. The elongation effect caused the stiffening of the spring due to the guitar string principle, where a string's stiffness increases as the tension in the string is increased. It was therefore important to clamp the ends of the spring elements to prevent any motion in the ends that would lessen the elongation of the spring and have a negative effect on the stiffening of the spring.

A design with straight springs was not suited to practical implementation on an isolator. Higher lateral stiffness and stability were needed, and in addition the straight spring caused a geometrical problem with implementation on the circular LIVE isolator. For this reason a circular spring was designed. These springs have a more consistent lateral stiffness in all directions. The clamping of the leaves was also much more effective because of the geometrically stiff circular shape of the outside of the spring. The circular spring consisted of inner and outer rings connected by three spokes. Two of these circular leaves were mounted on top of each other with the outside ring clamped in a frame and the leaves separated at the center.

4. STIFFNESS CONTROL

An automated actuation process was needed for the separation of the springs in order to change the stiffness of the spring while in operation. Smart materials, which are seen as materials with great potential that are still relatively unexplored, were considered as one option for separating the springs. Conceptually, such materials might yield a robust and simple mechanism for changing the stiffness of the spring without many moving parts. The problem with smart materials is that they do not provide a sufficient combination of force and stroke for the application, which typically requires forces of the order of a few hundred newtons with corresponding displacements of several millimeters.

Other actuators were therefore also considered, which would still have the objective of a simple robust separation mechanism. Finally, a wax actuator was selected owing to the large

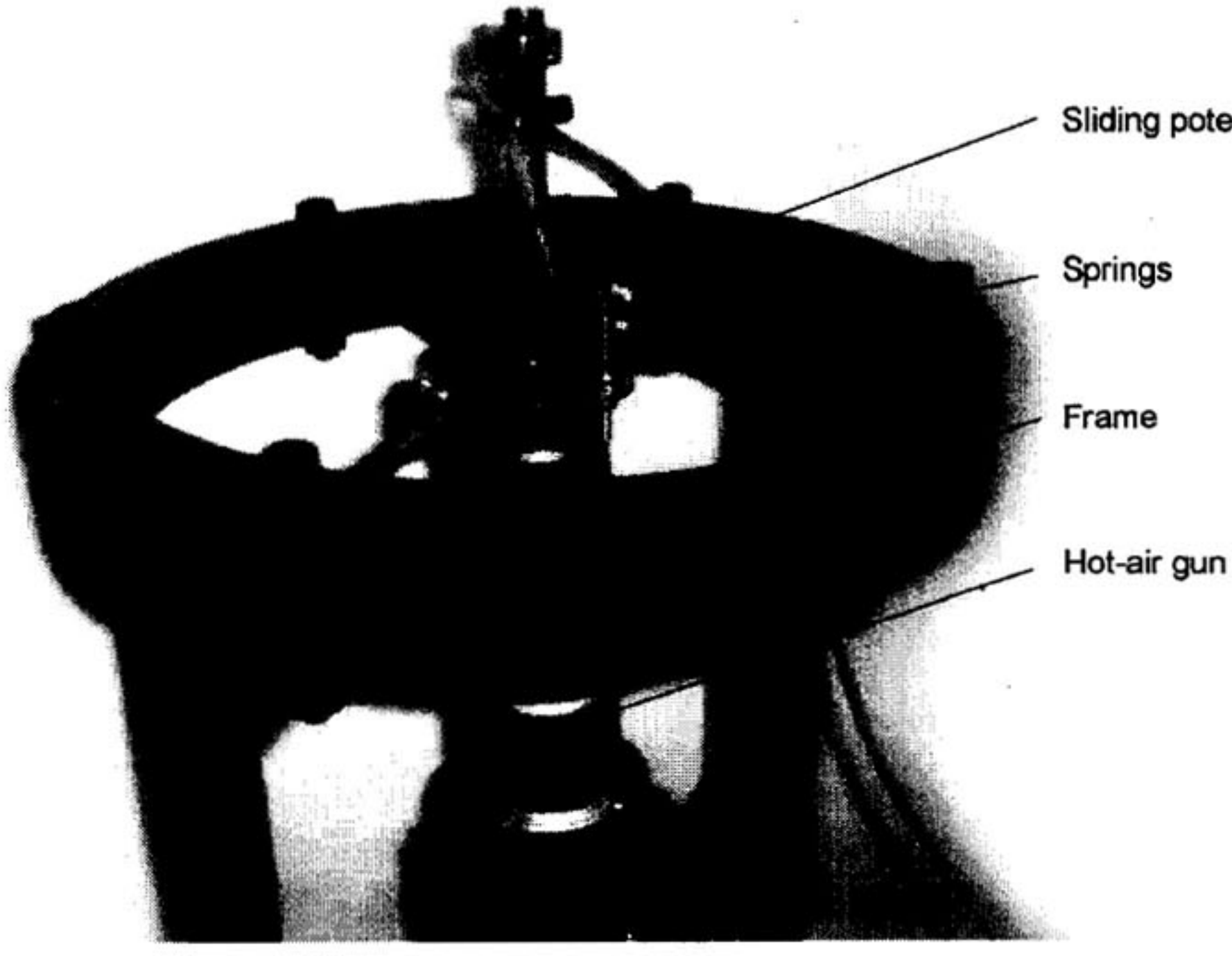

Figure 3. Experimental spring.

forces and displacements possible from a very compact actuator. These actuators employ the thermal expansion of a wax contained in a housing to displace an output shaft, and they are typically used in thermostats for automotive applications. A typical wax actuator can produce a force up to 500 N and provides a stroke length of 10 mm.

In this application, an external heating element was used in the form of a hot-air gun. The energy dissipation of the heating element was controlled with a computer-controlled DC-motor controller. The actuator was mounted by being sandwiched between the circular springs, so that the system could return to the original position of the actuator when the wax cooled down.

The displacement of the actuator had to be controlled so that the stiffness of the spring could be accurately controlled. A linear sliding potentiometer, measured with a computer, was used for position measurement on the system. The experimental spring assembly is shown in Figure 3.

The open-loop system was characterized by measuring time responses and deriving a Bode diagram. A second-order system model was fitted to it, as shown in Figure 4. The system may be described by an equation of the form

$$G(s) = \frac{\omega_n^2}{s^2 + 2\zeta\omega_n s + \omega_n^2}. \tag{9}$$

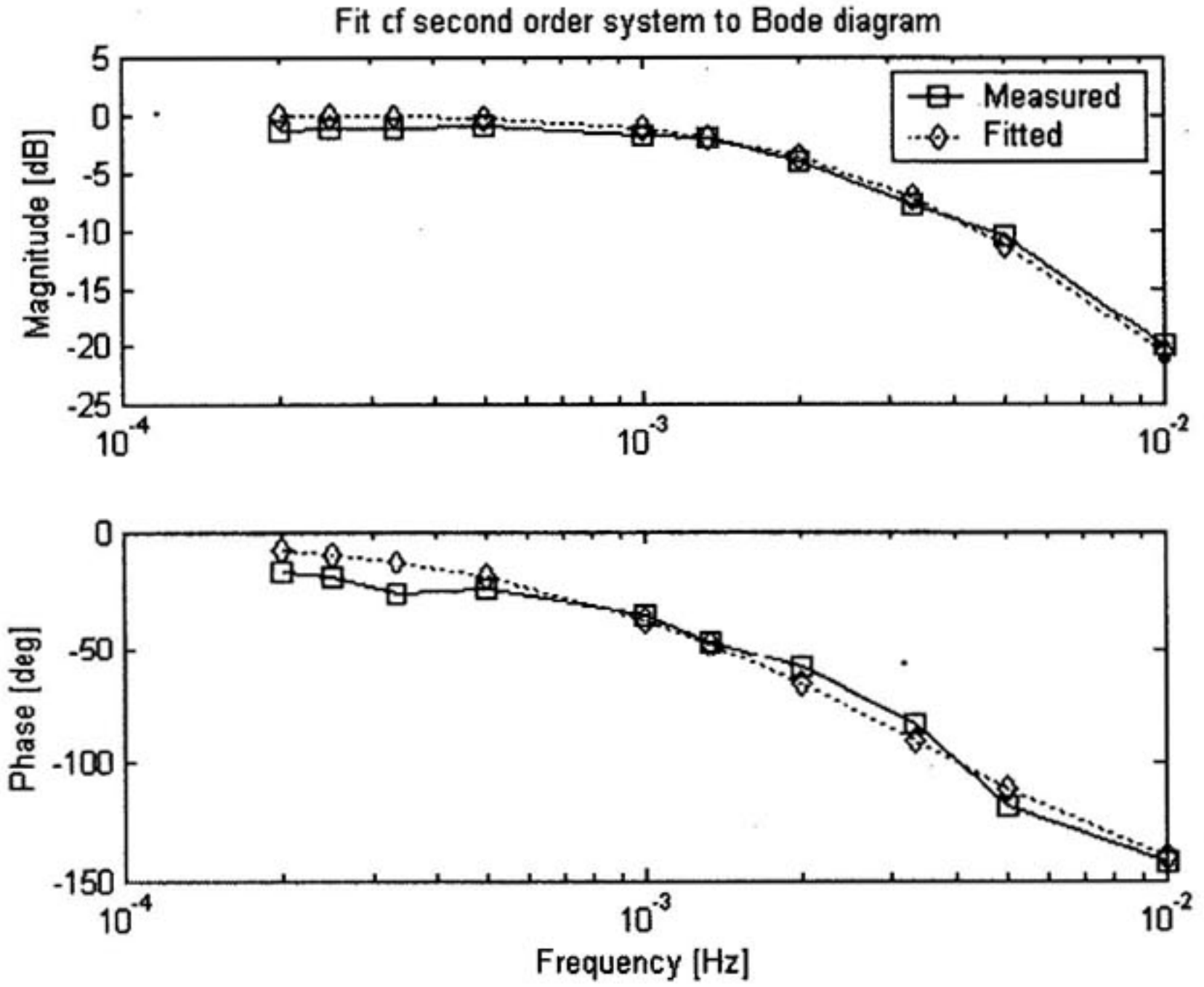

Figure 4. Bode diagram of the open-loop system.

Each point on the Bode diagram was measured by applying a single sinusoidal input to the open-loop system and measuring the corresponding displacement. Afterwards, the amplitude ratio and phase difference were determined and plotted on the Bode diagram. The second-order model representing the open-loop system was

$$G(s) = \frac{0.00046831}{s^2 + 0.046566s + 0.0004223}. \tag{10}$$

This corresponds to an overdamped second-order system with a natural frequency of 0.02055 rad s^{-1} and a damping ratio of 1.133.

The performance of the open-loop system was not satisfactory. The response time of the system was of the order of 120 s, and it was not possible to control the displacement of the system accurately. A much faster response time was needed with more accurate displacement control. For this reason, a closed-loop control system was used.

A computer, equipped with a National Instruments PCI 6024E 12-bit analog-to-digital converter (ADC) and a digital-to-analog converter (DAC), was used for the control. The displacement of the actuator was measured with the sliding potentiometer and the power consumption of the hot-air gun was controlled by using a DC-motor controller. The DC-motor controller was controlled by a 0–10 V DC signal from the DAC. The control algorithm, implemented in Matlab, made use of a displacement and velocity feedback closed-loop control system that resulted in an effective control system.

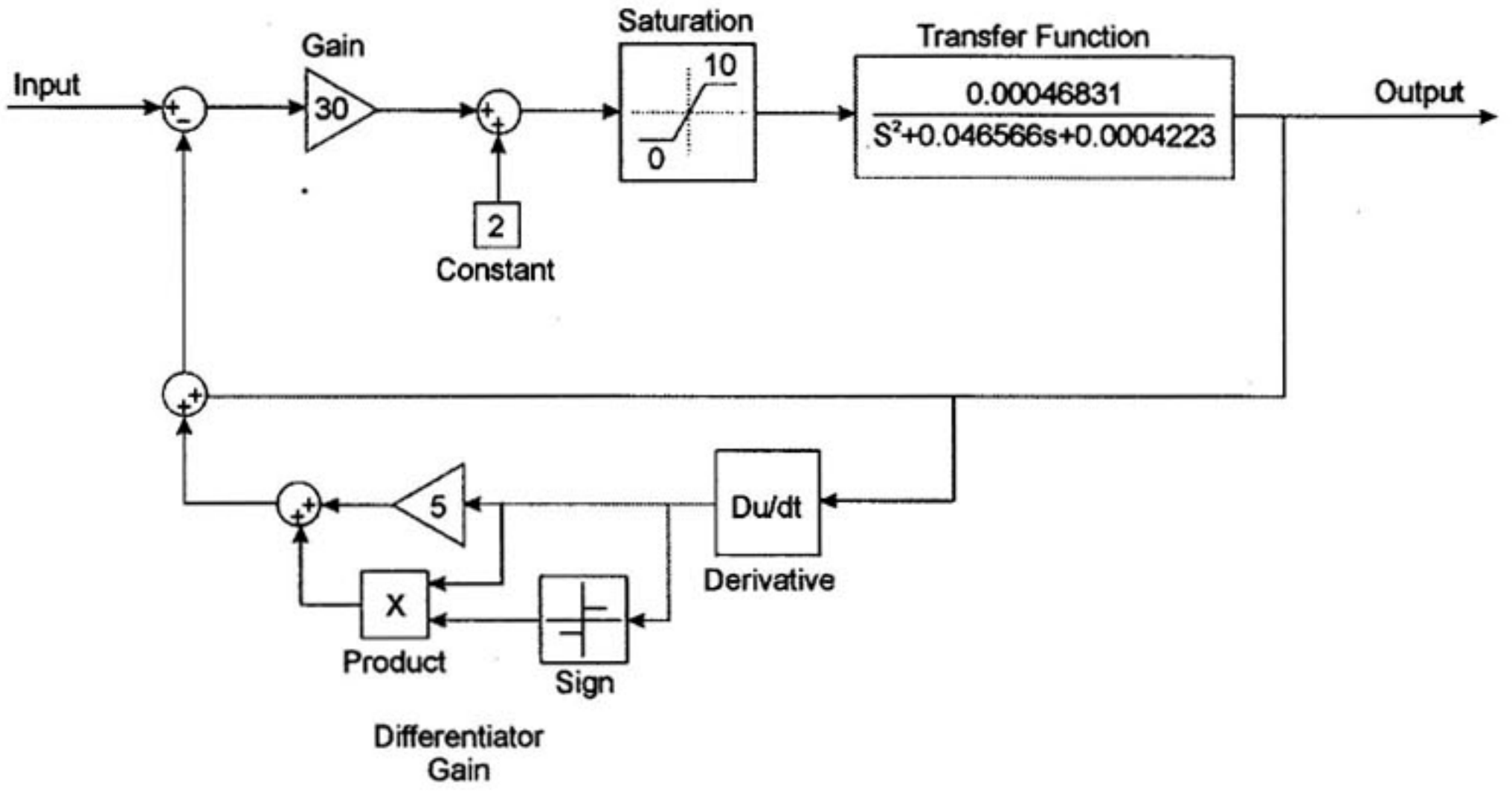

Figure 5. Block diagram of the closed-loop system.

Suitable gains were determined for the displacement and velocity feedback loops in the control system. A Simulink™ model of the system was constructed and is shown in Figure 5. This model incorporates all the practical constraints, such as bounded output voltage to the DC-motor controller of 0–10 V (implemented as a saturation) and DC offsets as well as the gains of the control system. The simulation yielded a response comparable to the response of the actual system. The closed-loop control system improved the performance of the system significantly and resulted in a response time of the order of 20 s. The closed-loop system fulfilled the requirements set for the application.

5. TESTING OF THE VARIABLE STIFFNESS SPRING

The complete spring assembly was used for determining the stiffness and damping of the spring. The spring was tested on an Excite ES 302-1 servo-hydraulic actuator. The actuator had a stroke length of 50 mm and a maximum force of 4900 N. The center of the spring was clamped with a load cell between the spring and the frame of the test table to measure the transmitted force. The frame clamping the outside ring of the springs was fixed to the servo-hydraulic actuator and moved up and down. The displacement of the actuator was measured with a strain gage displacement transducer. A sinusoidal signal of 10 Hz excited the spring and the displacement and force were measured. The two sensor signals were amplified with identical strain gage amplifiers to ensure an identical phase shift. The stiffness was determined as the amplitude ratio between the two signals. The damping was determined by calculating tan δ, where δ is the phase shift between the force and the displacement time signals. The results are given in Figure 6.

A stiffness change of 2.7 times the original stiffness was obtained by separating the springs by 8 mm. The structural damping of the spring had a loss factor of roughly 0.1. The

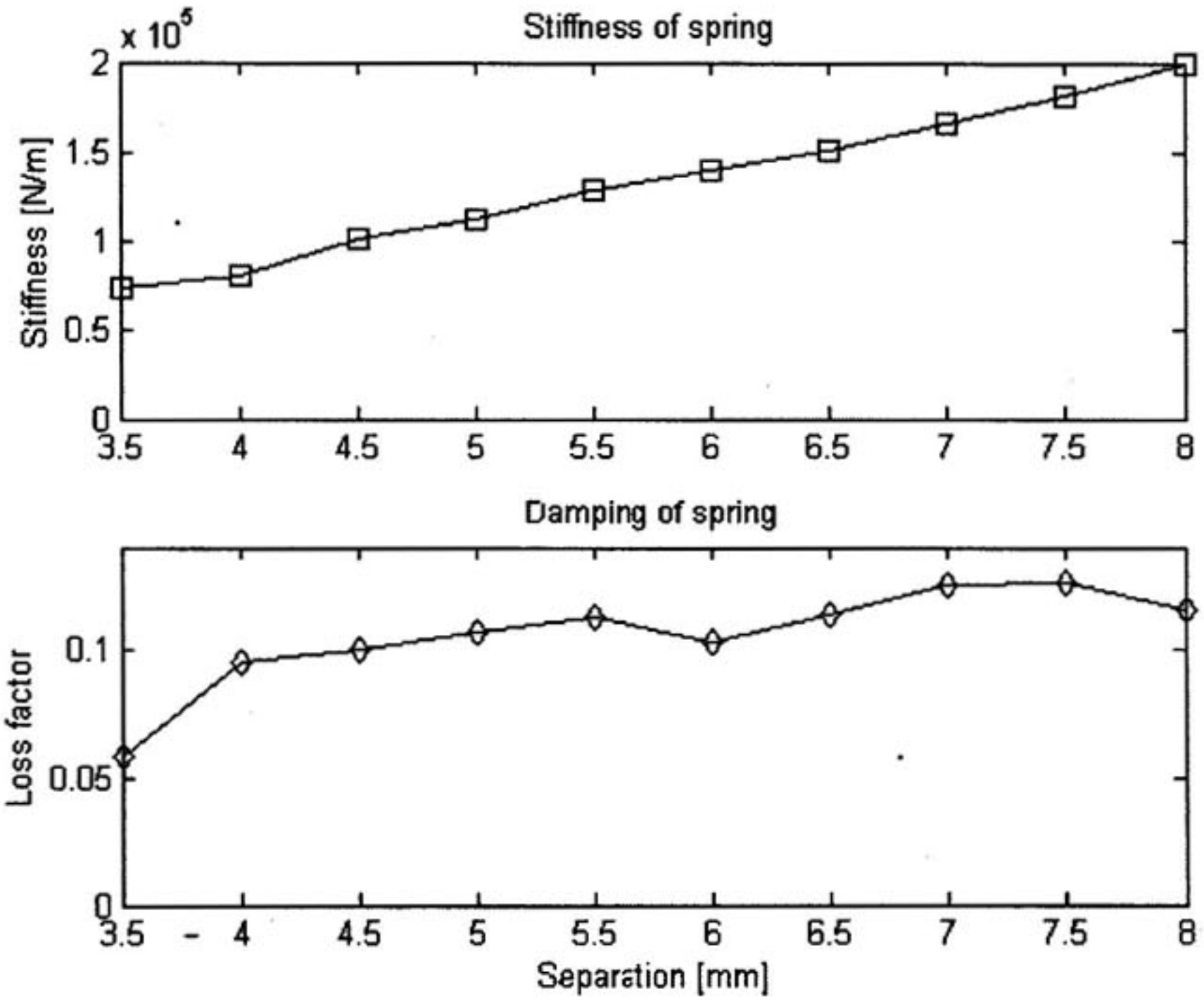

Figure 6. Stiffness and damping of the spring.

stiffness change of the spring fulfills the requirements set and will result in a sufficient shift in the isolation frequency of the isolator.

6. VARIABLE DAMPING

As mentioned in the introduction, the damping of the isolator needed to be altered during operation in some cases. Although the isolator is designed for perfect tonal excitation, it is foreseen that such an isolator can be used in an environment with a dominant excitation frequency, but with wide-band low-amplitude excitation over the whole frequency band. In such a case, the lowest possible damping will not yield the lowest possible transmitted vibration, as will be the case with perfect tonal excitation. The reason for this is the presence of a natural frequency of the isolator where the low-amplitude vibrations are amplified. It is therefore necessary in such cases to be able to change the damping of the isolator to achieve the lowest possible vibration transmission.

In the LIVE isolator, there are two sources of damping. The first is the structural damping of the spring element in the system and the second is the viscous damping from the flow losses in the port. In order to change the damping of the isolator, one or both of these two sources has to be altered. The structural damping of a spring is usually a property of the spring material and is quite difficult to change. By contrast, the flow losses in the port are a

function of the smoothness of the port and are very easy to change. Any flow disturbance or turbulent flow will increase the flow losses.

The high velocities of the fluid in the port make it even more suitable for the addition of damping. The higher the velocity of the fluid, the greater the flow losses and damping. In order to control the amount of damping, an obstruction has to be placed in the port that can be changed to vary the damping.

7. ISOLATOR DESIGN

Once the stiffness values of the variable stiffness spring are known, the rest of the LIVE isolator can be designed. An isolation frequency of 30 Hz, a port length of 100 mm, and a mass of 4 kg were chosen as parameters for the isolator.

An inherent problem in the design of a LIVE isolator is sealing the fluid inside the isolator. Usually an elastomer such as rubber is molded in between the inner and outer parts to seal the fluid inside and act as the spring in the system, but this is not possible in a case where an external variable stiffness spring is used. An effective solution was found by using rolling diaphragms (Simrit BFA 80 × 70 × 30) to seal the fluid inside the isolator while still allowing relative motion between the port and reservoir. The diaphragms worked well for this application. As the diaphragms had almost no stiffness of their own and only slight damping, this resulted in a design where almost any type of external spring could be implemented on the isolator. Therefore, the variable stiffness spring that was designed could be incorporated into the isolator without any degradation in the performance of the spring. The use of the rolling diaphragms eliminates most of the practical design constraints of a LIVE isolator and really opens the way for further research to develop any type of suitable external spring for this system. The diaphragms resulted in an effective reservoir diameter of 75 mm.

With these values known, equation (2) was used for determining the required port diameter. The port diameter was determined as 25 mm. The final design of the LIVE isolator is shown in Figure 7. The variable damping mechanism was a plate that could be rotated and was inserted into the port. The component consists of a flat center part with cylindrical ends that is used for rotation and sealing of the fluid inside the isolator. The component is positioned so that the flat plate falls inside the tuning port. By rotating the component, the angle of the plate relative to the flow of the water is changed. As the angle of the plate is changed, the flow losses of the water flowing over the plate increased, with maximum losses occurring when the surface of the plate was perpendicular to the flow direction of the water. The greater flow losses resulted in an increased damping of the isolator.

The isolator was tested on an Excite ES 302-1 servo-hydraulic actuator. The isolator was fixed to the actuator and was excited by using a random signal. Two 10 mV g^{-1} PCB accelerometers were used for measuring the response, one on the input (actuator) and the other on the outside of the isolator or output. The displacement transmissibility was determined with a Spectral Dynamics SigLab as the ratio between the output and the input in the frequency domain. The results for the different stiffness settings are shown in Figure 8. The stiffness was changed in steps from 75,000 to 200,000 N m^{-1} to obtain the given results. The isolation frequency shifted from 22.8 to 36.2 Hz. A transmissibility of less than 10% at the isolation frequency was obtained at all the settings. The effect of the variation in damping is

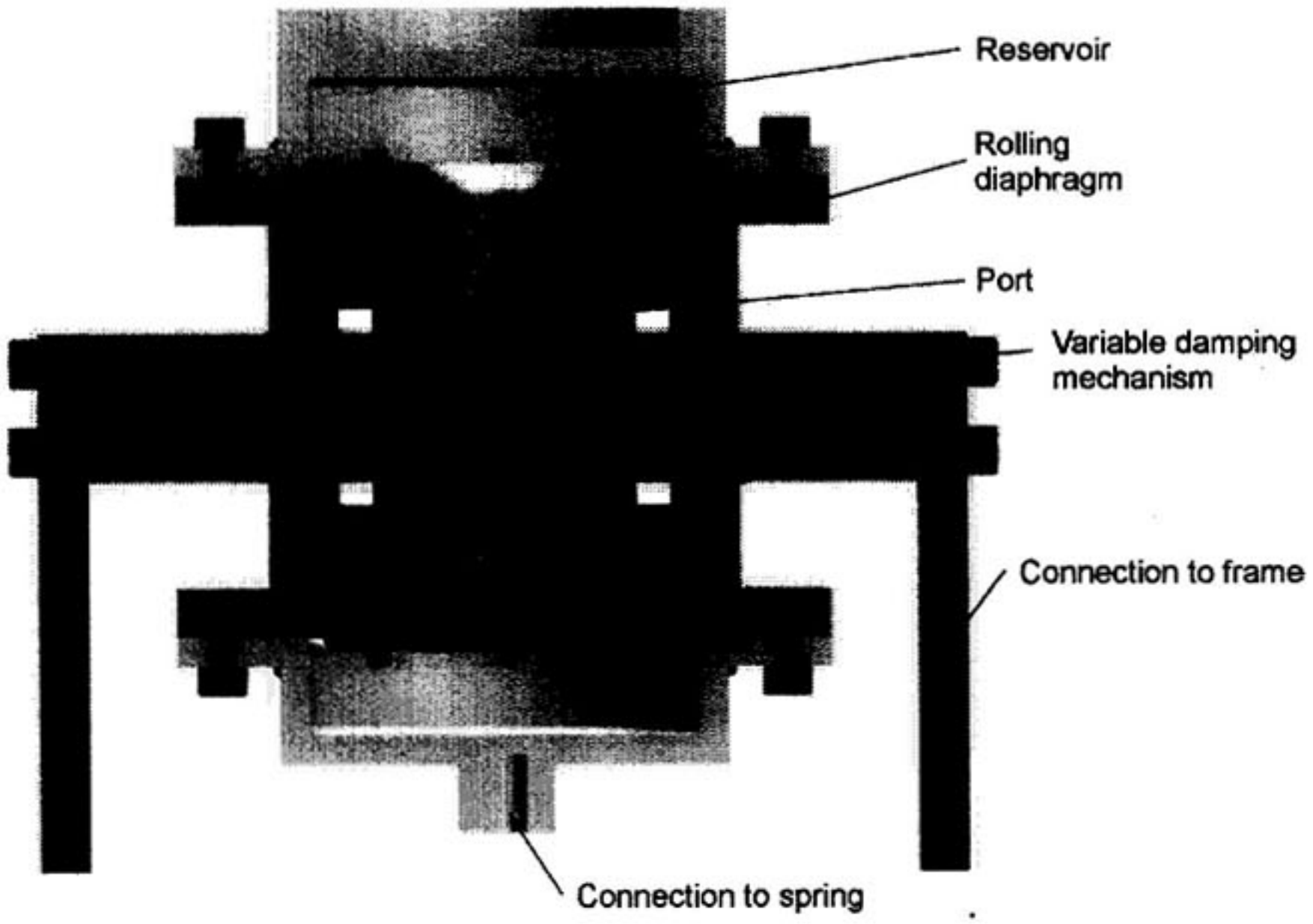

Figure 7. Design of the experimental isolator.

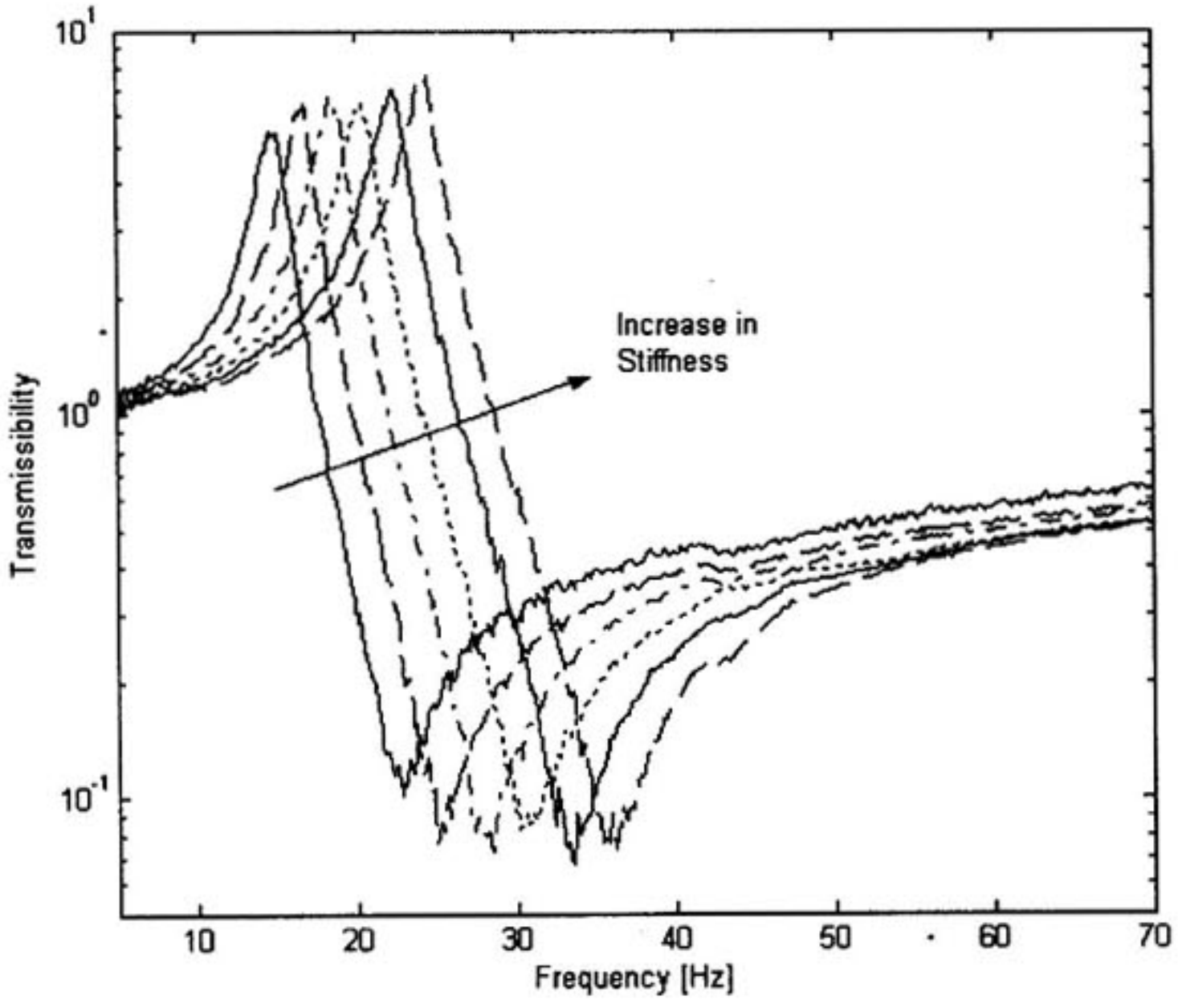

Figure 8. Transmissibility curves for different stiffness values.

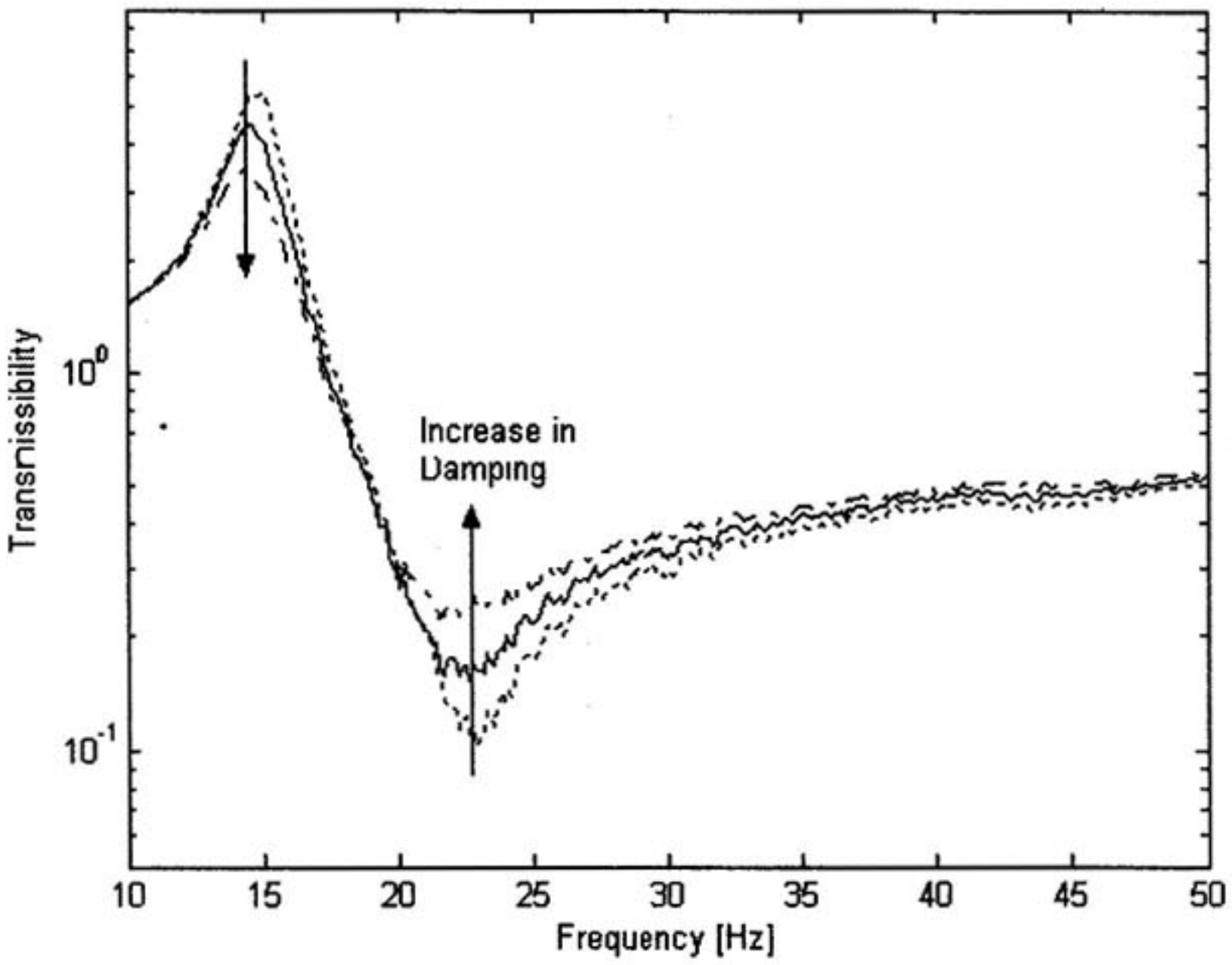

Figure 9. Transmissibility curves for different damping values.

shown in Figure 9. The transmissibility curves for the lowest stiffness setting and different damping settings are shown.

A least-squares curve fit method was used to fit the theoretical transmissibility curve given in equation (1) to the measured graphs. The values for the stiffness, structural damping, and viscous damping were determined by means of the curve fitting. Therefore these values represented the actual measured stiffness and damping values of the isolator. The fitted values for the stiffness of the isolator were almost identical to those measured on the spring in Figure 6, as could be expected. The viscous damping ratio changed from 0.001 to 0.033 for the different damping settings.

8. CONTROL SYSTEM FOR ISOLATOR

To demonstrate the automation of the process of tuning the isolator to the current excitation conditions, a control system was implemented on a computer that changed the stiffness automatically, using Matlab. The control system incorporated an optimization algorithm that minimized the root-mean-square (RMS) ratio. The RMS ratio can be calculated from the input and output acceleration time signals by using the following equation:

$$RMS_{Ratio} = \frac{RMS_{Output}}{RMS_{Input}}. \tag{11}$$

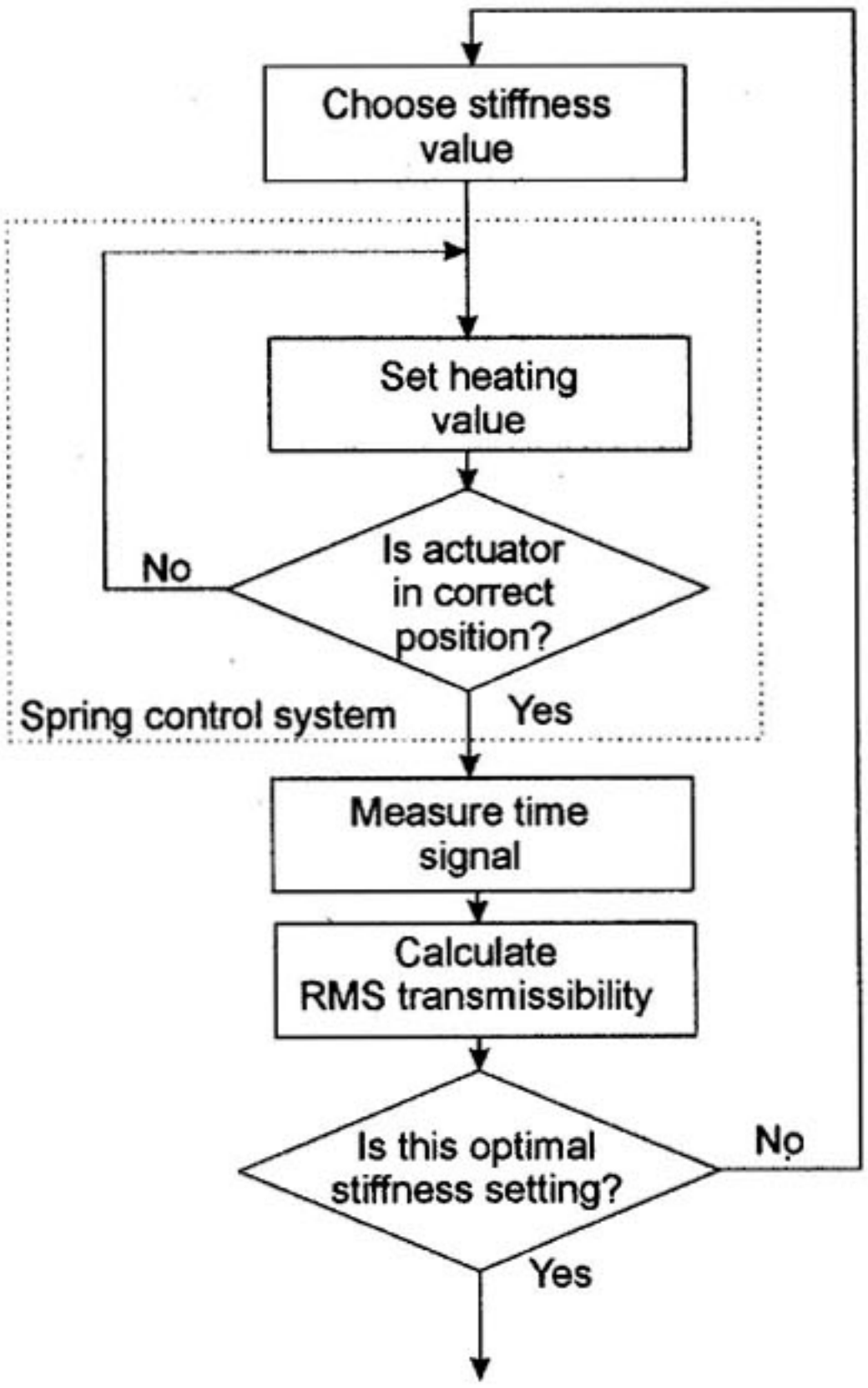

Figure 10. Block diagram of the optimization control system.

This value was minimized by changing the stiffness until the correct stiffness setting was obtained. The control system of the spring was incorporated into the algorithm. The optimization algorithm used was the Matlab function "Fminbnd", which is a scalar-bounded non-linear function minimization algorithm. The block diagram of the optimization control system is depicted in Figure 10. The convergence of the optimization control system, for excitation frequencies ranging from 24 to 32 Hz, is shown in Figure 11. Each line on the graph represents a certain excitation frequency and gives the RMS ratio values for each iteration in the optimization process. It can be seen that the optimization program converged within 12 iterations each time. The peak at the second iteration of some of the lines is due to the boundaries that are evaluated by the optimization algorithm. The algorithm was bounded by the stiffness range of the spring, and the system was evaluated at the boundaries to interpolate between these values. The control system optimized the spring to a minimum RMS ratio that represents the minimum transmission of forces to the isolated structure.

When the optimum settings were determined, the control system kept the isolator at those settings and monitored the RMS ratio value. The reason is that a change in the excitation conditions causes an increase in the RMS ratio. As soon as the RMS ratio increased, the

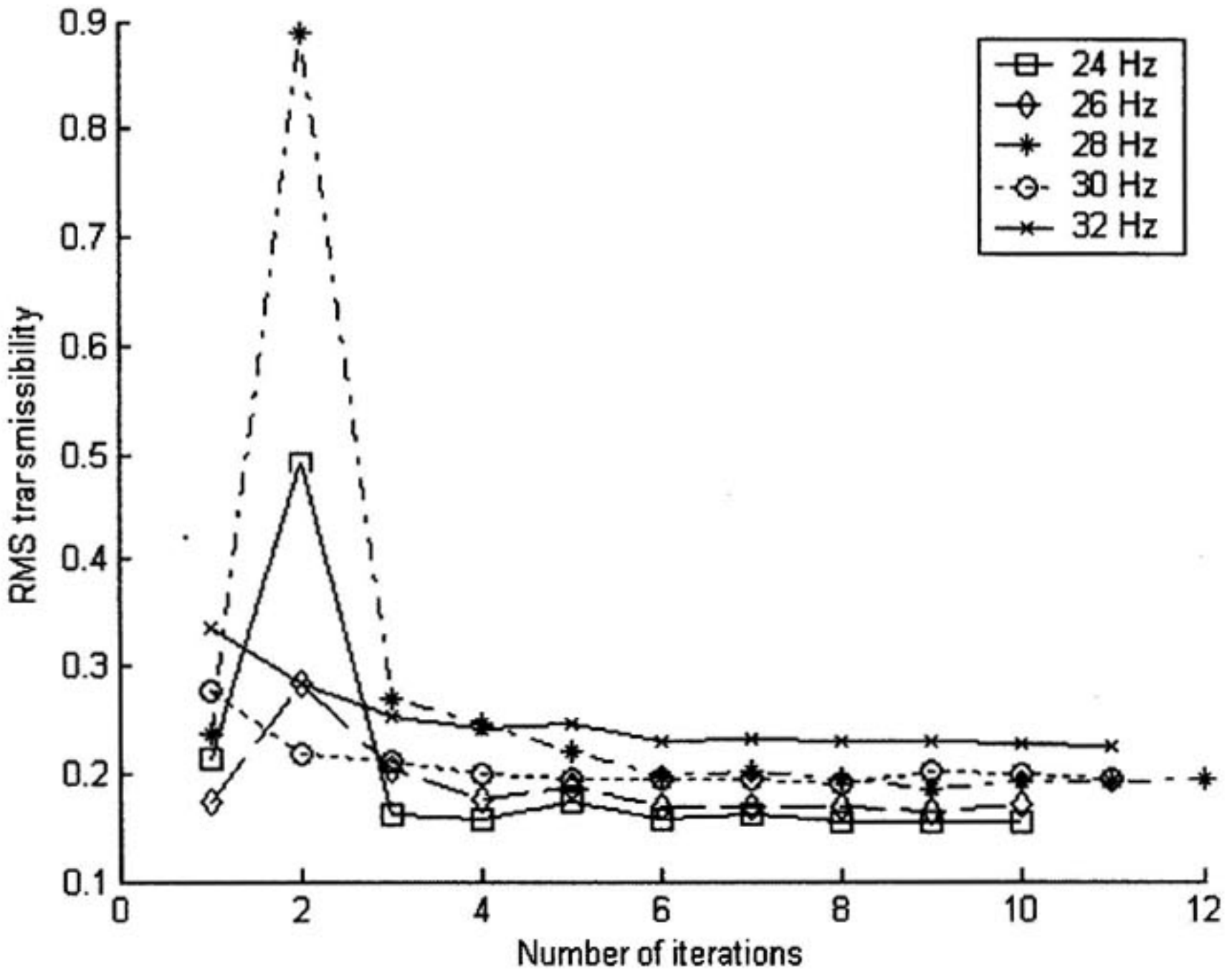

Figure 11. Convergence graphs of the optimization control system.

optimization was started again from the beginning. The same principle could be used to control the damping setting. The optimization would then become a two-variable optimization problem.

9. CONCLUSION

A tunable vibration isolator was developed using the LIVE concept. For this purpose, a variable stiffness spring was developed, using a wax actuator to separate the leaves of a circular compound leaf spring. This resulted in an increase of 270% in the original stiffness. Correspondingly, the isolation frequency of the isolator was shifted by 58% from 22.8 to 36.2 Hz. A variable damping mechanism was also implemented, which changed the viscous damping ratio of the isolator from 0.001 to 0.033.

A closed-loop displacement and velocity feedback control system was implemented to prove that it is practical to automate the tuning of the isolator.

The use of rolling diaphragms as seals in the LIVE isolator opens possibilities for the use of various external spring configurations on this type of isolator. The study has also shown the potential of wax actuators, and future work could improve the time response of the actuators by using faster heating and cooling techniques.

Acknowledgment. The authors gratefully acknowledge the financial support for this work provided by the Council for Scientific and Industrial Research (CSIR) in South Africa.

REFERENCES

Braun, D., 1980, "Development of antiresonance force isolators for helicopter vibration reduction," in *Sixth European Rotocraft and Powered Lift Aircraft Forum*, Bristol, UK, September 16–19, Paper no. 18, pp. 1–17.

Brennan, M. J., Elliot, S. J., and Long, T., 1996, "Automatic control of multiple vibration neutralisers," *Proceedings of Inter-Noise* **96**, 1597–1602.

Desjardins, R. A. and Hooper, W. E., 1976, "Rotor isolation of the hingeless rotor B0-105 and YUH-61A helicopters," in *2nd European Rotorcraft and Powered Lift Aircraft Forum*, Buckeburg, Germany, September, Paper no. 13, pp. 1–13.

Desjardins, R. A. and Hooper, W. E., 1980, "Antiresonant rotor isolation for vibration reduction," *Journal of the American Helicopter Society* **25**(3), 46–55.

Du Plooy, N. F., 1999, *The Development of a Vibration Absorber for Vibrating Screens*, M. Eng. Thesis, University of Pretoria, South Africa.

Flannelley, W. G., 1966, "The dynamic antiresonant vibration isolator," in *22nd Annual AHS National Forum*, Washington, DC, pp.153–158.

Franchek, M. A., Ryan, M. W., and Bernhard, R. J., 1995, "Adaptive passive vibration control," *Journal of Sound and Vibration* **189**(5), 565–585.

Halwes, D. R. and Simmons, W. A., 1980, "Vibration suppression system," US Patent Specification Number 4,236,607.

Halwes, D. R., 1981, "Total main rotor isolation system analysis," Bell helicopter textron, *NASA Contractor Report No. 165667*, Langley Research Center, Hampton, VA, June.

Hodgson, D. A. and Duclos, T. G., 1991, "Vibration isolator with electrorheological fluid controlled dynamic stiffness," US Patent Specification Number 5,029,823.

Longbottom, C. J. and Rider, M. J. D. E., 1987, "A self-tuning vibration absorber," UK Patent Specification Number GB 2189573 B.

Ribakov, Y. and Gluck, J., 1998, "Optimal design of base isolated active controlled MDOF structures," in *International Conference on Noise and Vibration Engineering, ISMA23*, Leuven, Belgium, September.

Rita, A. D., McGarvey, J. H., and Jones, R., 1976, "Helicopter rotor isolation utilizing the dynamic antiresonant vibration isolator," in *32nd Annual AHS National Forum*, Washington, DC, May, pp. 22–29.

Siler, D. and Demoret, K. B., 1996, "Variable stiffness mechanisms with SMA actuators," *Proceedings of the SPIE* **2721**, 427–435.

Smith, K. E., 1991, "Smart tuned mass dampers," in *Proceedings of ADPA/AIAA/ASME/SPIE Conference on Active Materials and Adaptive Structures,* Alexandria, VA, November.

Smith, M. R. and Stamps, F. B., 1995, "Vibration isolation system," US Patent Specification Number 5,435,531.

Smith, M. R. and Stamps, F. B., 1998, "Vibration isolation system," US Patent Specification Number 5,788,029.

Von Flotow, A. H., Beard, A., and Bailey, D., 1994, "Adaptive tuned vibration absorbers: Tuning laws, tracking agility, sizing, and physical implementations," in *Proceedings of Noise-Con 94*, Fort Lauderdale, FL, May, pp. 437–454. .

Walsh, P. L. and Lamancusa, J. S., 1992, "A variable stiffness vibration absorber for the minimization of transient vibrations," *Journal of Sound and Vibration* **158**(2), 195–211.